Semiconductor Physics, Quantum Electronics & Optoelectronics, 2025. V. 28, No 3. P. 284-291.

Semiconductor physics

Parameter determination of ion-implanted layers of single crystals by integrated dynamical diffractometry

G.I. Nyzkova[1], B.M. Romanyuk[2], O.V. Dubikovskyi[2], O.Yo. Gudymenko[2], O.A. Kulbachynskyi[2], A.O. Bilotska[1], T.P. Vladimirova[1], Ya.V. Vasylyk[1], O.S. Skakunova[1], I.I. Demchik[1], L.I. Makarenko[1], S.V. Lizunova[1], I.M. Zabolotny[1], V.V. Molodkin[1], O.S. Kononenko[1], V.V. Lizunov[1]

[1]*G.V. Kurdyumov Institute for Metal Physics, NAS of Ukraine,*
36 Academician Vernadsky Boulevard, 03142 Kyiv, Ukraine
[2]*V. Lashkaryov Institute of Semiconductor Physics, NAS of Ukraine, 41 Nauky Avenue, 03028 Kyiv, Ukraine*
[*]*Corresponding author e-mail: nizkova@imp.kiev.ua*

Abstract. X-ray diffraction methods are highly informative for investigation of crystal structure imperfections. They are widely applied to determine the characteristics of structural defects in various materials. In this work, by processing experimentally measured azimuthal dependences of the total integrated intensity of dynamical diffraction for three asymmetric Bragg reflections for a Si single crystal irradiated with boron ions, the thicknesses of the amorphous absorbing surface layer and the kinematically scattering layer as well as the concentration of randomly distributed dislocation loops in the dynamically scattering volume located under the above-mentioned disturbed surface layers are obtained.

Keywords: phase variation diagnostics, azimuthal dependence, defects.

https://doi.org/10.15407/spqeo28.03.284
PACS 07.85.Jy, 61.72.uf

Manuscript received 10.04.25; revised version received 04.08.25; accepted for publication 03.09.25; published online 24.09.25.

1. Introduction

Materials with quantum dots are widely used in advanced electronic devices such as photodetectors, LEDs, lasers, memory elements, *etc*. [1]. Quantum dots are solid nanoparticles in the form of precipitates or inclusions of new phases that have a discrete spectrum of electronic states depending on their size. Ion implantation is also used for creating nanoprecipitates buried in a solid matrix. This process leads to self-organization effects such as separation of the precipitate ensembles (see, *e.g.* [2–6]). The development of an ensemble of precipitates in a solid solution goes through the stages of nucleation, growth of all precipitate nuclei from the solution, and, finally, passes to the stage of Ostwald ripening, when the concentration in the solution decreases approaching the equilibrium value, and the growth of some precipitates occurs due to the dissolution of the neighboring, smaller precipitates [7, 8]. The interaction between the precipitates at the Ostwald ripening stage explains the creation of ordered nanoparticle ensembles based on self-organization effects [9–13], which is one of the most important tasks of nanotechnology.

Because of ion bombardment during boron implantation in silicon, structural transformations such as formation of a highly disordered (amorphized) thin surface layer as well as formation and accumulation of radiation defects, are possible. Subsequent annealing or repeated ion implantation causes recrystallization in the highly disordered (amorphized) thin surface layer. In the technology of manufacturing photovoltaic cells, control of the parameters of both the initially amorphized and recrystallized layers is important.

Implantation and subsequent annealing lead to significant transformations of the X-ray rocking curves compared to the rocking curves of the original sample. In [14], influence of the magnitude and shape of the strain distribution in the surface layers of single crystals, *i.e.*, the relative change $\Delta d/d$ of the interplanar distance normal to the surface with respect to the substrate, on the shape of the two-crystal Bragg reflection curves was experimentally discovered and studied, and a method for restoring the strain distribution profile over depth was developed based on the semi-kinematical scattering theory. It was established [14, 15] that the depth of the maximum deformation increases with the implantation energy. As the implantation dose increases, the height of the maximum deformation and its integral value proportionally increase.

In addition to the deformation profiles in alloyed materials, it is also necessary to determine the statistical characteristics of microdefects randomly distributed within the bulk. For example, it is known that Czochralski grown (CZ) Si single crystals, even after growth, contain

large dislocation loops with an average radius R = 20 μm and small dislocation loops with an average radius R = 0.02 μm. It was shown in [16] that boron implantation into silicon leads to formation of dislocation loops.

Determining the structure of solids using advanced tri-axial diffractometry methods by measuring the distribution of the diffracted intensity in the reciprocal lattice space requires measuring low intensities differentially at each point of the reciprocal space. Use of integrated parameters allows a significant reduction of the measuring time and increase of the diagnostics precision. In the works of M.O. Krivoglaz [17], the defects were classified according to the nature of their influence on the kinematical pattern of scattering. Both Bragg and diffuse scattering were described in the kinematical approximation. However, the total integrated reflection intensity at kinematical diffraction does not depend on the degree of distortion of the crystal lattice. Hence, for kinematically scattering crystals with defects, methods based on measuring total integrated scattering intensities are not suitable.

Additional opportunities are provided by using a dynamical scattering pattern instead of a kinematical one. The integrated characteristics of the dynamical scattering pattern are more sensitive to structural imperfections. At the same time, measuring and processing the dependences of the total integrated intensity of dynamical diffraction (TIIDD) on the diffraction conditions allows quantitative determination of the characteristics of the defect structure of single crystals [18].

The aim of this work is to clarify the possibilities of determining the parameters of the defect structure of single crystals irradiated with boron ions using the method of azimuthal dependences (AD) of TIIDD.

2. AD TIIDD theoretical model for a single crystal with a disordered surface layer and randomly distributed defects

The studied crystal is divided into three zones: (1) non-diffracting absorbing 'amorphous' layer with the thickness t_{am} (disordered surface layer – DSL), (2) stressed zone with the thickness $t_{k.s.l.}$, and (3) dynamically scattering single crystal containing randomly distributed defects (RDD) [20]. The total integrated intensity of dynamical diffraction of the three-layer system is

$$R_i = \left(R_i^{RDD} + R_{i\,ks}\right)\exp\left\{-\mu_0\left[t_{am} + k\Lambda\left(\frac{a}{d}\right)\right]\left(\frac{a}{\gamma_0} + \frac{1}{|\gamma_H|}\right)\right\},$$

$$R_i^{RDD} = R_i^{dyn.} PE + R_{iP}\Pi\left(1 - E^2\right),$$

$$R_{i\,ks} = C^2\left(\frac{Q}{\gamma_0}\right) t_{kp\,c} = C^2\left(\frac{Q}{\gamma_0}\right) k\Lambda\left(\frac{a}{d}\right).$$

Here, C is the polarization factor, $Q = \left(\pi|\chi_{Hr}|\right)^2 / \left[\lambda\sin(2\theta)\right]$ is the reflectivity per unit path length, χ_{Hr} is the real part of the Fourier component of the crystal polarizability, t is the crystal thickness, γ_0 and γ_H are the direction cosines of the wave vectors of a plane wave incident on a crystal relative to the internal normal to the input surface of the crystal and the diffracted wave, respectively, and μ_0 is the linear photoelectric absorption coefficient.

The Krivoglaz–Debye–Waller factor $L_H = -\ln E$ is [17]

$$L_H \approx 0.5c\upsilon_c^{-1}R_0^3(Hb)^{3/2}.$$

Here, υ_c is the volume of a unit cell of the matrix, R_0 is the average radius of the dislocation loops, c is the dislocation loop concentration, **b** is the Burger vector, **H** is the diffraction vector, and

$$R_i^{dyn.} = \left(\frac{16}{3\pi}\right) CQ\Lambda/\gamma_0,\ R_{i\,P} = \frac{C^2 Qt}{\gamma_0},$$

$$\Pi\left(\mu^*, t\right) = \frac{1}{\left[\frac{2\left(\mu_0 + \mu^*\right)t}{\gamma}\right]},\ \frac{1}{1/\gamma} = \frac{1}{2}\left(\frac{1}{\gamma_0} + \frac{1}{|\gamma_H|}\right),$$

$$P \cong 1 - 3\frac{\pi s}{4} \text{ at } s << 1,\ s = \left(\mu_0 + \mu_{ds}^0\right)\frac{\Lambda E}{\gamma C}.$$

The directional cosines are calculated by the following expressions:

$$\gamma_0 = -\cos\theta_B \sin\psi\cos\varphi + \sin\theta_B\cos\psi,$$
$$\gamma_H = -\cos\theta_B \sin\psi\cos\varphi - \sin\theta_B\cos\psi,$$

where ψ is the angle between the reflecting planes and the crystal surface, and φ is the azimuth angle, respectively.

For RDD of the Coulomb type with the radius R_0 and concentration c [19]

$$\mu_{ds}^0 = cE^2C^2m_0B,\ m_0 = \frac{\pi\upsilon_c H^2|\chi_{Hr}|^2}{2\lambda^2},$$

$$B = b_1 + b_2\ln\left(\frac{e}{r_0^2}\right),\ b_1 = B_1 + \frac{B_2}{3},\ b_2 = B_1 + \cos^2\theta_B\frac{B_2}{2},$$

where $r_0 = \frac{R_0}{\Lambda}$ and $\Lambda = \lambda\sqrt{\gamma_0\gamma_H}\left(C|\chi_{Hr}|\right)$ is the extinction length under assumption $r_0 < 1$.

For randomly distributed dislocation loops

$$B_1 = \frac{4\left(\frac{\pi b R_0^2}{\upsilon_c}\right)}{15},\ B_2 = \beta B_1,\ \beta = \left(3\nu^2 + 6\nu + 1\right)/\left[4\left(1 - \nu^2\right)\right],$$

where ν is the Poisson ratio.

If $\mu_{ds}^0 << \mu_0$ and $r_0 << 1$, $\mu^* \approx \mu_{ds}^0 f_\mu(r_0)$, $f_\mu(r_0) = \left(5 + 2r_0\ln r_0 - 3/8r_0\right)/\left[3\left(1 - \ln r_0\right)\right]$.

Hence, the parameters E, μ_{ds}^0 and μ^* and, consequently, TIIDD R_i interrelate with the RDD characteristics (c, R_0, b).

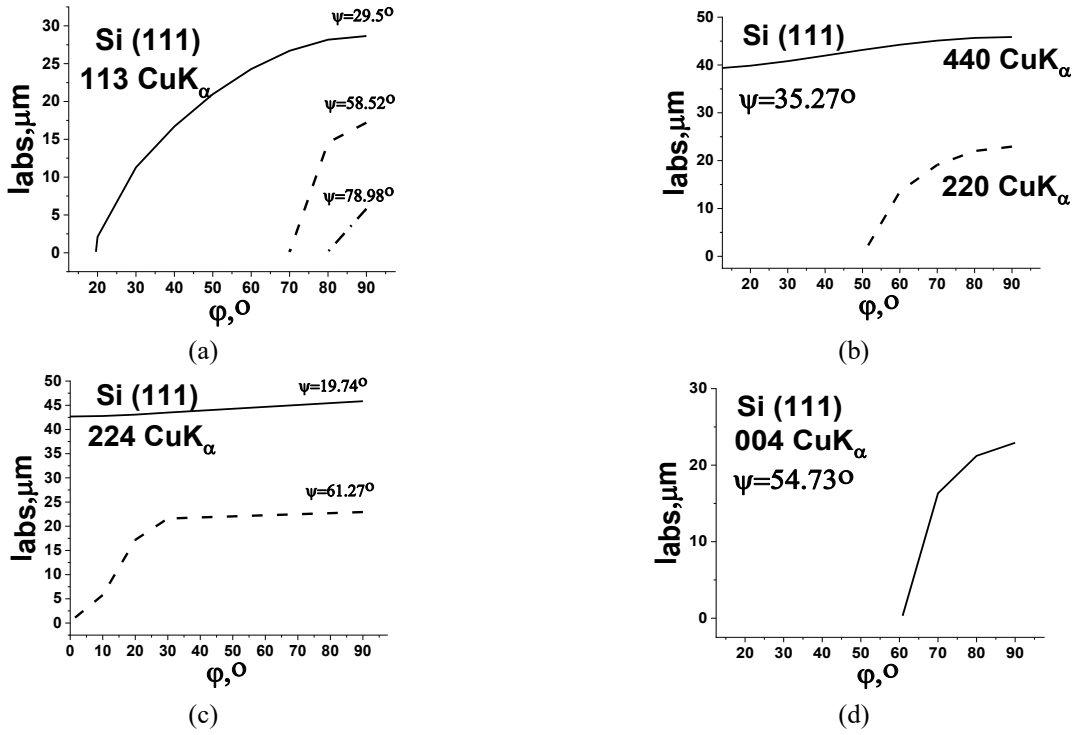

Fig. 1. AD of the penetration depth of X-rays into the studied single crystal.

3. Determination of DSL characteristics by the AD TIIDD method

The DSL parameters were characterized by the AD TIIDD method at Bragg asymmetric diffraction. In particular, the penetration depth of X-rays into the studied crystal at different asymmetric reflections was investigated. The presented experimental results were obtained using a Panalytical Philips X'Pert PRO diffractometer (V. Lashkaryov Institute of Semiconductor Physics, NAS of Ukraine) (λ_{CuK} = 1.5406 Å) equipped with high resolution X-ray optics, namely a Ge (220) monochromator and a double Ge (220) analyzer. The studied Si sample was irradiated with boron ions at a dose of 10^{12} atoms/cm^2 and ion energy of 400 keV.

The AD of the penetration depth for various reflections of the (111) Si samples were calculated. The calculations presented in this article were done for Si single crystals with microdefects according to the models proposed in [20, 21]. The calculation results are shown in Fig. 1.

Fig. 1 shows that the penetration depth almost does not depend on the azimuth angle for the angles between the reflecting planes and the crystal surface $\psi << \theta_B$ (Figs. 1b and 1c). At the same time, the penetration depth at large angles ψ significantly decreases (almost to ~ 0.3 μm).

X-rays total external reflection is used at angles less than the critical angle $\theta_c = \sqrt{2\delta}$. The relative decrement of refraction δ for X-rays with the wavelength λ ~ 1 Å and carbon-containing compounds is 10^{-6}. For real systems with absorption, the dependence on the angle is smooth. In particular, diffraction of X-ray beams incident on the surface of a crystal at a small angle $\Phi_0 \le 1$ and Φ_0 close to $\Phi_c = \sqrt{|\chi_0|}$ is studied (here, χ_0 is the polarization). For silicon, Φ_c = 13.35′ = 0.2225°. It should be noted that study of grazing dynamical X-ray diffraction in perfect single crystals [22, 23] and single crystals with defects [24] is widely used.

In this work, diffractometric measurements were carried out for the minimum penetration depths of X-rays, which corresponded to the angles $\arcsin\left(\sqrt{\gamma_0\gamma_H}\right) > 0.2225°$. For example, for asymmetric (220) reflection at φ = 128.3°, $\arcsin\left(\sqrt{\gamma_0\gamma_H}\right) = 0.805° \approx 3.6\,\Phi_c$.

Implantation of boron ions in a silicon single crystal leads to formation of an amorphous absorbing layer, the thickness of which increases with the ion energy. According to the proposed model, an elastically stressed kinematically scattering layer with the thickness proportional to the extinction length with a proportionality coefficient k is formed between this absorbing layer and the dynamically scattering volume. At $t_{am} = l_{abs}\Big/\sqrt{\gamma_0|\gamma_H|}$, there is no diffraction in the crystal and the intensity of the incident X-rays only decays compared to that for a perfect crystal with $t_{am} = 0$.

It should be noted that at $t_{am} << l_{abs}$, TIIDD of a single crystal is the sum of the kinematic and dynamical terms attenuated in the absorbing layer.

For investigation of the sensitivity of the TIIDD to the characteristics of the DSL at different reflections, the dependences of the TIIDD on the radiation penetration depth $l_{abs}(\varphi)$ into a crystal with the DSL parameters k = 0.033 at t_{am} = 0.1 μm [19, 25, 26] were calculated. The calculation results are presented in Fig. 2.

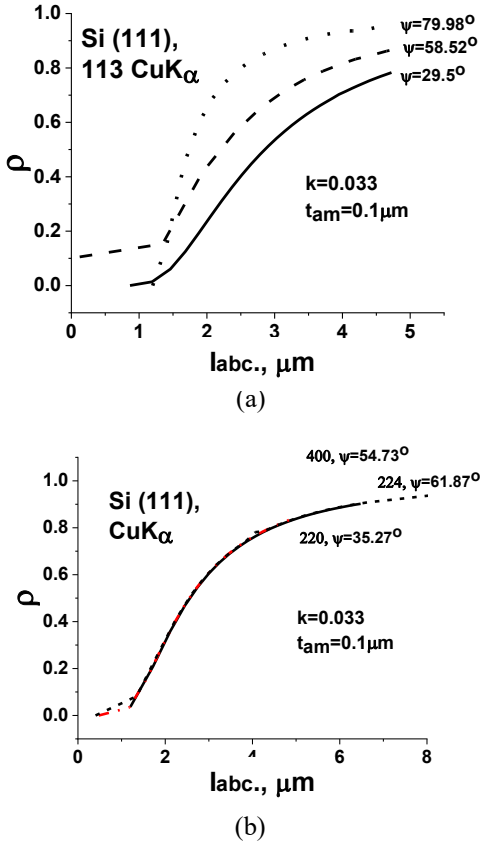

Fig. 2. Dependences of the TIIDD R_i of a crystal with a DSL normalized to the IIDD of a perfect crystal, $R_{perf.cr}$ ρ = = $R_i/R_{perf.cr}$, on the absorption depth l_{abs} of CuKα radiation: reflection (113) (*a*), and reflections (400), (220) and (224) (*b*).

As can be seen from Fig. 2a, the dependences for the reflection (113) at ψ = 29.5°, 58.52° and 79.98° are substantially different because of the difference in the maximum penetration depths: $l_{abs.max}$ (ψ = 29.5°) = 28.66 μm, $l_{abs.max}$ (ψ = 58.52°) = 17.19 μm and $l_{abs.max}$ (ψ = 79.98°) = 5.73 μm. In Fig. 2b, the dependences for the reflections (220), (400) and (224) are similar, because the maximum penetration depths for these reflections are equal, $l_{abs.max}$ = 22.93 μm.

4. Diagnostics of defect structure of a single crystal containing three defect types by the AD TIIDD method

Measurements of the AD TIIDD for the original and irradiated samples were performed for the reflections (224) CuK$_\alpha$ (ψ = 19.47°), (220) CuK$_\alpha$ (ψ = 35.27°) and (115) CuK$_\alpha$ (ψ = 70.5289°).

It was shown that for the (224) CuK$_\alpha$ reflection (ψ = 19.47°), the maximum absorption depth is $l_{abs.max}$ = 45.86 μm and the maximum extinction depth is Λ_{max} = 15.48 μm; for the (220) CuK$_\alpha$ reflection (ψ = 35.27°), the maximum absorption depth is $l_{abs.max}$ = 22.93 μm and the maximum extinction depth is Λ_{max} = 5.64 μm; for the (115) CuK$_\alpha$ reflection (ψ = 70.5289°), the maximum absorption depth is $l_{abs.max}$ = 17.20 μm and the maximum extinction depth is Λ_{max} = 8.64 μm. The experimental and calculated AD TIIDD are shown in Fig. 3. Here, the markers ▪ are the experimentally measured AD TIIDD for the original Si single crystal and the markers ● are the experimentally measured AD TIIDD for the Si single crystal irradiated with B ions. The solid line is the AD TIIDD calculated taking into account the influence of the DSL and RDD, the dashed line is the AD TIIDD calculated taking into account the influence of only the amorphous absorbing sub-layer of the DSL, the dashed-dotted line is the AD TIIDD calculated taking into account the influence of only the DSL, and the dotted line is the AD TIIDD calculated taking into account the influence of only the RDD.

Comparison of the experimental AD TIIDD for the original and irradiated samples shows a significant difference between the AD TIIDD of the irradiated single crystal measured for different reflections. As shown below, this effect is caused by predominant manifestation of different defect types under different diffraction conditions on the TIIDD.

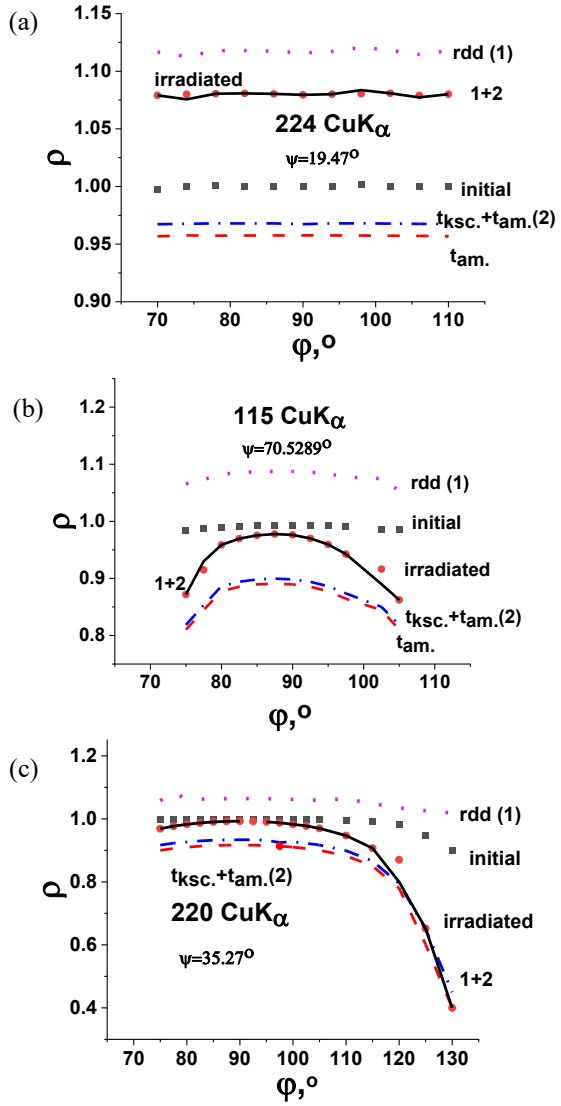

Fig. 3. AD of the TIIDD normalized to the IIIDD of the perfect crystal: reflection (224) (a), reflection (115) (b), and reflection (220) (c).

Fig. 3a shows that the measured values of the normalized TIIDD are almost equally far from the calculated values both in the presence of only RDD and only DSL in the irradiated sample. Figs 3b and 3c demonstrate that the measured values of the normalized TIIDD are close to the calculated values in the presence of only DSL in the irradiated sample. In this case, account of both defect types makes the calculation results coincide with the experiment.

Comparison of the ADs of the TIIDD calculated for the cases of presence of only an absorbing layer in the irradiated single crystal and presence of both absorbing and kinematically scattering layers shows that the influence of the kinematically scattering layer more strongly compensates the influence of the absorbing layer for quasi-symmetric (115) reflection than for strongly asymmetric (220) reflection. This is due to the fact that the ratio of the absorption length to the extinction length in the second case is larger. Therefore, strongly asymmetric reflection (220) is selectively sensitive to the amorphous absorbing layer, the quasi-symmetric reflection (115) is selectively sensitive to the kinematically scattering layer, and the reflection (224) is selectively sensitive to the RDD.

By processing the experimental data for three above-mentioned reflections for the ion-irradiated sample, the following values of the defect structure parameters are obtained: the concentration of randomly distributed dislocation loops with the radius $R = 0.02$ μm is equal to $c = 5\cdot10^{13}$cm^{-3} ($c/\upsilon_c = 2.5\cdot10^{-10}$), the thickness of the amorphous absorbing surface layer $t_{am} = 1$ μm, and the thickness of the kinematically scattering surface layer $t_{ksc} = k\Lambda(a/d)$, $k = 0.08$. Therefore, $t_{ksc}(115,\ \varphi = 90°) = 44.923\cdot0.08 = 3.6$ μm, $t_{ksc}(220,\ \varphi = 90°) = 15.941\cdot0.08 = 1.3$ μm, and $t_{ksc}(224,\ \varphi = 90°) = 75.826\cdot0.08 = 6$ μm.

For analyzing the experimental results from [14], the value of the IIDD ratio for a perfect crystal $R_{perf.cr}$ to the TIIDD R_i for the ion-irradiated crystal, $1/\rho_{\exp} = R_{perf.cr}/R_{i\exp}$, is suggested to use to quantitatively characterize deformation of the crystal lattice. Fig. 4 shows the dependence $\ln\left(\frac{1}{\rho_{\exp}}\right)(l_{abs})$ calculated using the experimental data obtained for reflection (220).

Fig. 5 shows the deformation profiles from [14] and the calculated profile $0.03\ln(1/\rho_{\exp})(l_{abs})$. Here, the coefficient 0.03 is chosen by fitting. It should be mentioned that the main interest is to the relative positions of the profile maxima (dependent on the implantation energy), not their dose-dependent heights.

It can be seen from Fig. 5 that the maximum stress values qualitatively correspond to the energy values of boron ions during implantation.

Experimental depth distributions of boron implanted at a dose of 10^{15} $^{11}B^+$ ions cm^{-2} and an energy of 400 keV into amorphous, polycrystalline, and monocrystalline silicon, obtained by secondary-ion mass spectrometry (SIMS) also had maxima at the depth of 1 μm [27].

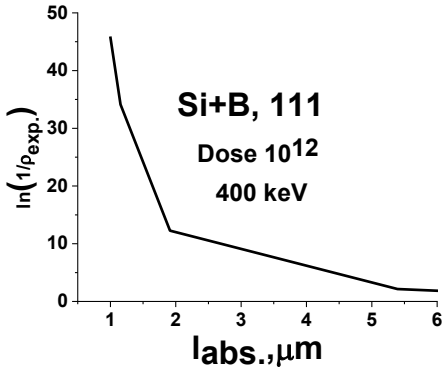

Fig. 4. $\ln(1/\rho_{\exp})$ *versus* absorption depth l_{abs} for boron-doped silicon.

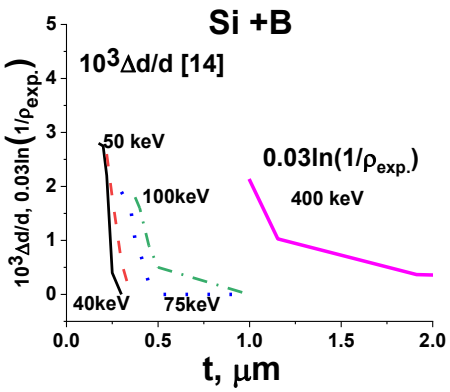

Fig. 5. Stress profiles in boron-doped silicon.

5. Conclusions

The optimal conditions of Bragg asymmetric diffraction for diagnosing defects in boron-implanted silicon single crystal are found. Namely, reflection (220) is selectively sensitive to the amorphous absorbing layer parameters, reflection (115) is selectively sensitive to the kinematically scattering layer parameters, and reflection (224) is selectively sensitive to RDD in the dynamically scattering volume.

The values of the thicknesses of the absorbing and kinematically scattering DSL and the concentration of small randomly distributed dislocation loops are also obtained.

It is shown that the ratio of the depth dependence of stress calculated for a perfect crystal to the experimental TIIDD is similar to the stress profiles obtained earlier from the rocking curves, and the maximum stress corresponds to the energy of boron ions during implantation.

References

1. *Semiconductor Nanostructures for Optoelectronic Applications*, Ed. Steinen T., Boston-London, Artech House, 2004.
2. Lagzi I., Kowalczyk B., Grzybowski B.A. Liesegang rings engineered from charged nanoparticles. *J. Am. Chem. Soc.* 2010. **132**, No 1. P. 58–60. https://doi.org/10.1021/ja906890v.

3. Lagzi I., Kowalczyk B., Wang D., Grzybowski B.A. Nanoparticle oscillations and fronts. *Angew. Chem. Int. Ed*. 2010. **49**, Issue 46. P. 8616–8619. https://doi.org/10.1002/anie.201004231.
4. Evans J.H. Observations of a regular void array in high purity molybdenum irradiated with 2 MeV nitrogen ions. *Nature*. 1971. **229**. P. 403–404. https://doi.org/10.1038/229403a0.
5. Sckerl M.W. *et al*. Precipitate coarsening and self organization in erbium-doped silica. *Phys. Rev. B*. 1999. **59**. P. 13494–13497. https://doi.org/10.1103/PhysRevB.59.13494.
6. Mohr C., Dubiel M., Hofmeister H. Formation of silver particles and periodic precipitate layers in silicate glass induced by thermally assisted hydrogen permeation. *J. Phys.: Condens. Matter*. 2001. **13**. P. 525–536. https://doi.org/10.1088/0953-8984/13/3/312.
7. Reiss S., Heinig K. H. Ostwald ripening during ion beam synthesis a computer simulation for inhomogeneous systems. *Nucl. Instrum. Methods Phys. Res. B.* 1994. **84**. P. 229–233. https://doi.org/10.1016/0168-583X(94)95760-6.
8. Tishkovsky E., Feklistov K., Taskin A., Zatolokin M. Influence of amorphization-recrystallization processes on distribution of selenium and oxygen atoms implanted in silicon. *Vacuum*. 2003. **70**. P. 153–156. https://doi.org/10.1016/S0042-207X(02)00634-6.
9. Reiss S., Heinig K.H. Self-structuring of buried SiO_2 precipitate layers during IBS: A computer simulation. *Nucl. Instrum. Methods Phys. Res. B.* 1995. **102**. P. 256. https://doi.org/10.1016/B978-0-444-82410-3.50051-5.
10. Karpov V.G., Grimsditch M. Large-scale fluctuations in the diffusive decomposition of solid solutions. *Phys. Rev. B*. 1995. **51**. P. 5181–5200. https://doi.org/10.1103/PhysRevB.51.8152.
11. Maksimov L.A., Ryazanov A.I., Heinig K.H., Reiss S. Self-organization of precipitates during Ostwald ripening. *Phys. Lett. A*. 1996. **213**. P. 73. ttps://doi.org/10.1016/0375-9601(96)00092-8.
12. Reiss S., Weber R., Heinig K.H., Skorupa W. Experimental study and modeling of structure formation in buried layers at ion beam synthesis. *Nucl. Instrum. Methods Phys. Res. B*. 1994. **89**. P. 337. https://doi.org/10.1016/0168-583X(94)95195-0.
13. Borodin V.A., Heinig K.H., Reiss S. Self-organization kinetics in finite precipitate ensemles during coarsening. *Phys. Rev. B*. 1997. **56**. P. 5332–5344. https://doi.org/10.1103/PhysRevB.56.5332.
14. Kyutt R.N., Petrashen P.V., Sorokin L.V. Strain profiles in in-doped silicon obtained from X-Ray rocking curves. *phys. status solidi (a)*. 1980. **60**. P. 381. https://doi.org/10.1002/pssa.2210600207.
15. Liu J., Krishnamoorthy V., Gossman H.J. The effect of boron implant energy on transient enhanced diffusion in silicon. *J. Appl. Phys.* 1997. **81**, No 4. P. 1656. https://doi.org/10.1063/1.364022.
16. Razak N.E.A., Dee C.F., Madhuku M. *et al.* Role of boron in assisting the super-enhancement of emissions from carbon implanted silicon. *Materials*. 2023. **16**. P. 2070. https://doi.org/10.3390/ma16052070.
17. Krivoglaz M.A. *X-Ray and Neutron Diffraction in Nonideal Crystals*. Berlin, Springer, 1996. https://doi.org/10.1007/978-3-642-74291-0.
18. Lizunov V.V. *et al.* Integrated diffractometry: achieved progress and new performance capabilities. *Usp. Fiz. Met.* 2019. **20**, No 1. P. 75. https://doi.org/10.15407/ufm.20.01.075.
19. Molodkin V.B., Nizkova A.I., Shpak A.P. *et al. Diffractometry of Nanosized Defects and Heterolayers of Crystals*. Kyiv, Akademperiodyka, 2005.
20. Molodkin V.B., Olikhovskii S.I., Dmitriev S.V. *et al.* Dynamical effects in the integrated X-ray scattering intensity from imperfect crystals in Bragg diffraction geometry. I. Semi-dynamical model. *Acta Cryst.* 2020. A**76**. P. 45–54. https://doi.org/10.1107/S2053273319014281.
21. Molodkin V.B., Olikhovskii S.I., Dmitriev S.V., Lizunov V.V. Dynamical effects in the integrated X-ray scattering intensity from imperfect crystals in Bragg diffraction geometry. II. Dynamical theory. *Acta Cryst.* 2021. A**77**. P. 433–452. https://doi.org/10.1107/S2053273321005775.
22. Afanas'ev A.F., Melkonyan M.K. X-ray diffraction under specular reflection conditions. Ideal crystals. *Acta Cryst. A*. 1983. **39**. P. 207. https://doi.org/10.1107/S0108767383000471.
23. Sakata O., Hashizume H. Dynamical X-ray diffraction profiles for asymmetric reflection form crystals under grazing incidence conditions. *Jpn. J. Appl. Phys.* 1988. 27, No 11. P. L1976. https://doi.org/10.1143/JJAP.27.L1976.
24. Radchenko T.M., Tatarenko V.A., Lizunov V.V. *et al.* Defect-pattern-induced fingerprints in the electron density of states of strained graphene layers: diffraction and simulation methods. *phys. status solidi (b)*. 2019. **256**. P. 1800406 (8 p.). https://doi.org/10.1002/pssb.201800406.
25. Molodkin V.B., Storizhko V.Yu., Kladko V.P. *et al.* New possibilities for phase-variation structural diagnostics of multiparametrical monocrystalline systems with defects. *SPQEO.* 2021. **24**. P. 5–15. https://doi.org/10.15407/spqeo24.01.005.
26. Molodkin V.B., Storizhko V.Yu., Kladko V.P. *et al.* Integrated dynamical phase-variation diffractometry of single crystals with defects of three and more types. *SPQEO.* 2023. **26**. P. 17–24. https://doi.org/10.15407/spqeo26.01.017.
27. Hofker W.K. *Implantation of Boron in Silicon*. Amsterdam, Stellingen, 1975.

Authors and CV

Hanna I. Nyzkova, Doctor of Sciences (Physics and Mathematics), Professor, Leading Researcher at the Department of Physics for Multiparametrical Structural Diagnostics of the G. Kurdyumov Institute for Metal Physics. Author of more than 100 publications. Her research interests include solid-state physics, dynamical theory of diffraction, and integrated diffractometry.
https://orcid.org/0000-0003-2942-6729

Boris M. Romanyuk, DSc in Physics and Mathematics, Professor, Head of the Department of Ion-Beam Engineering and Structural Analysis of the V. Lashkaryov Institute of Semiconductor Physics. Author of more than 270 scientific publications. His research interests include physics of semiconductors and dielectrics, ion-beam engineering and wide-range studies of semiconductor structures.
E-mail: romb@isp.kiev.ua,
https://orcid.org/0000-0002-1688-7588

Oleksandr Dubikovskyi, PhD in Physics and Mathematics, Researcher at the Department of Ion-Beam Engineering and Structural Analysis of the V. Lashkaryov Institute of Semiconductor Physics. He is the author of more than 16 publications. The main directions of his scientific activity are ion-beam modification and mass-spectrometry of semiconductor structures. E-mail: dubikovsky_o@ukr.net,
https://orcid.org/0000-0002-1504-8440

Oleksandr Yo. Gudymenko, PhD, Senior Researcher at the Department of Ion-Beam Engineering, V. Lashkaryov Institute of Semiconductor Physics. Author of more than 60 publications. Field of research: solid-state physics, dynamical theory of diffraction of radiation, X-ray optics,and X-ray diffraction analysis of semiconductor crystals. E-mail: gudymen@ukr.net,
https://orcid.org/ 0000-0002-5866-8084

Oleksandr A. Kulbachynskyi, PhD Student at the Department of Ion-Beam Engineering and Structural Analysis of the V. Lashkaryov Institute of Semiconductor Physics. His main research activities are physics of thin films, chromogenic materials, SIMS analysis and ion implantation.
E-mail: s.kulbachynskyi@gmail.com,
https://orcid.org/0000-0001-6657-5569

Alla O. Bilotska, PhD in Physics and Mathematics, Senior Researcher at the Department of Physical Foundations of Diagnostics and Radiometry of Materials of the G. Kurdyumov Institute for Metal Physics. Author of more than 40 publications. Her research interests include solid-state physics and X-ray diffraction analysis of materials.
E-mail: aabel@imp.kiev.ua,
https://orcid.org/0009-0001-0914-6140

Tatyana P. Vladimirova, PhD in Physics and Mathematics, Head of the Laboratory of Physics for Multiparametrical Structural Diagnostics of the G. Kurdyumov Institute for Metal Physics. Author of more than 50 publications. Her research interests include solid-state physics, dynamical theory of diffraction, phase-contrast imaging, coherent X-ray diffractive imaging. E-mail: angelsgift@ukr.net,
https://orcid.org/0009-0005-2342-0256

Yaroslav V. Vasylyk, PhD in Physics and Mathematics, Senior Researcher at the Laboratory of Physics for Multiparametrical Structural Diagnostics of the G. Kurdyumov Institute for Metal Physics. Author of more than 30 publications. His research interests include solid-state physics and X-ray diffraction analysis of materials. E-mail: vasylyk@imp.kiev.ua,
https://orcid.org/0009-0005-1169-8787

Olena S. Skakunova, PhD in Physics and Mathematics, Researcher at the Department of Physical Foundations of Materials Diagnostics and Radiometry of the G. Kurdyumov Institute for Metal Physics. Author/co-author of more than 40 publications. Her research interests include dynamical theory of diffraction and structural diagnostics of film and multilayered structures.
E-mail: eskakunova007@gmail.com

Iryna I. Demchyk, PhD in Physics and Mathematics, Researcher at the Department of Physics for Multiparametrical Structural Diagnostics of the G. Kurdyumov Institute for Metal Physics. Author of more than 20 publications. Her research interests include methods of the total integrated intensities in the dynamical theory. E-mail: rudnytskaya@ukr.net,
https://orcid.org/0000-0002-2490-0869

Lyudmyla I. Makarenko, PhD in Physics and Mathematics, Junior Researcher at the Laboratory of Physics for Multiparametrical Structural Diagnostics of the G. Kurdyumov Institute for Metal Physics. Author of more than 11 publications. Her research interests include solid-state physics, methods of the total integrated intensities in the dynamical theory, and phase-variation diagnostics.
E-mail: makarenko_lyudmila@ukr.net,
https://orcid.org/0009-0000-0294-4695

Svitlana V. Lizunova, PhD in Physics and Mathematics, Senior Researcher at the Laboratory of Physics of Multiparametrical Structural Diagnostics of the G. Kurdyumov Institute for Metal Physics. Author of more than 50 publications. Her research interests include solid state physics, theory of phase-contrast imaging, and dynamical diffraction theory.
E-mail: svetlana.lizunova@gmail.com,
https://orcid.org/0009-0000-8434-1299

Ivan M. Zabolotnyi, PhD in Physics and Mathematics, Researcher at the Department of Physical Foundations of Diagnostics and Radiometry of Materials, G. Kurdyumov Institute for Metal Physics. Author of more than 18 publications. His research interests include solid-state physics, X-ray diffraction analysis of materials, and high performance computing.

Vitalii V. Molodkin, PhD in Physics and Mathematics, Researcher at the Laboratory of Physics for Multiparametrical Structural Diagnostics of the G. Kurdyumov Institute for Metal Physics. Author of more than 20 publications. His research interests include dynamical theory of diffraction and integrated diffractometry.
E-mail: molodkinvitaliy@gmail.com

Olga S. Kononenko, PhD in Physics and Mathematics, Junior Researcher at the Laboratory of Physics for Multiparametrical Structural Diagnostics of the G. Kurdyumov Institute for Metal Physics. Author of more than 15 publications. Her research interests include solid-state physics and X-ray diffraction analysis of materials. E-mail: kononenkoo289@gmail.com,
https://orcid.org/0009-0004-3130-6085

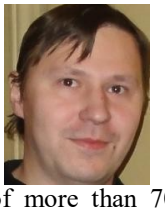

Vyacheslav V. Lizunov, Doctor of Sciences (Physics and Mathematics), Head of the Department of Physics for Multiparametrical Structural Diagnostics of the G. Kurdyumov Institute for Metal Physics. Author of more than 70 publications. His research interests include solid-state physics, dynamical theory of diffraction, phase-contrast imaging, coherent X-ray diffractive imaging, and strongly correlated materials.
E-mail: lizunov.vyacheslav@gmail.com,
https://orcid.org/0000-0002-3264-0219

Authors' contributions

Nyzkova H.I., Bilotska A.O., Vladimirova T.P., Vasylyk Ya.V., Skakunova O.S., Demchyk I.I., Makarenko L.I., Lizunova S.V., Kononenko O.S.: processing of experimental data, visualization, writing – review & editing.
Romanyuk B.M.: data analysis, investigation.
Dubikovskyi O.V.: investigation, visualization.
Gudymenko O.Yo: data analysis, investigation.
Kulbachynskyi O.A.: investigation, visualization.
Zabolotny I.M.: software, visualization.
Molodkin V.V.: theoretical analysis, software.
Lizunov V.V.: theoretical analysis, writing – original draft, writing – review & editing.

Визначення параметрів імплантованих іонами шарів монокристалів методом інтегральної динамічної дифрактометрії

Г.І. Низкова, Б.М. Романюк, О.В. Дубіковський, О.Й. Гудименко, О.А. Кульбачинський, А.О. Білоцька, Т.П. Владімірова, Я.В. Василик, О.С. Скакунова, І.І. Демчик, Л.І. Макаренко, С.В. Лізунова, І.М. Заболотний, В.В. Молодкін, О.С. Кононенко, В.В. Лізунов

Анотація. Рентгенодифракційні методи є високоінформативними для дослідження недосконалостей кристалічної структури. Вони широко застосовуються для визначення характеристик дефектів структури в різноманітних матеріалах. У цій роботі шляхом обробки експериментально виміряних азимутальних залежностей повної інтегральної інтенсивності динамічної дифракції для трьох асиметричних Брегг відбиттів від монокристала кремнію, опроміненого іонами бору, отримано значення товщин аморфного поглинаючого поверхневого шару та кінематично розсіюючого шару, а також концентрації рівномірно розподілених дислокаційних петель у динамічно розсіюючому об'ємі під вищевказаними порушеними поверхневими шарами.

Ключові слова: фазоваріаційна діагностика, азимутальна залежність, дефекти.